Emerging Cutting-Edge Developments in Intelligent Traffic and Transportation Systems
M. Shafik (Ed.)

doi:10.3233/ATDE240024

High-Speed Localization Estimation Method Using Lighting Recognition in Tunnels

Yushi MOKO [a], Yuka HIRUMA [b], Tomohiko HAYAKAWA [a,b,1], Yoshimasa ONISHI [c] and Masatoshi ISHIKAWA [a]

[a] *Tokyo University of Science, Japan*
[b] *The University of Tokyo, Japan*
[c] *Central Nippon Expressway Company Limited, Japan*

Abstract. This study proposes a vision-based high-speed localization estimation method for location based visual inspection of specific cracks in tunnels on Japanese expressways where global navigation satellite systems are not applicable. The method relies on recognizing lighting facilities installed in tunnels by using random sample consensus (RANSAC), enabling stable and accurate localization estimation in the horizontal direction. To correspond with traveling at high speed, single instruction/multiple data (SIMD) conversion realized 8 times faster than conventional image processing. The evaluation experimental results on expressway demonstrate that the proposed method achieves a maximum error of 31 mm in estimating lighting facilities position with an average error of 16 mm. The theoretical value derived from tunnel completion drawings has a maximum difference of 177 mm from the total value by this method, indicating that the results of accurate on-site measurements should be prioritized over completion drawings. In conclusion, the proposed method has considerable potential for practical application in tunnel inspection and maintenance.

Keywords. Localization estimation, Infrastructure inspection, Tunnel, Lighting facilities, High-speed camera, Japanese expressways, Crack

1. Introduction

At the end of March 2021, more than half of Japanese total expressway length, measuring at 9,231.7 km, had been in service for over 30 years [1]. Maintaining the safety of deteriorated infrastructure by conducting appropriate repairs and updates is more cost-effective than rebuilding expressways [2]. In this regard, detailed inspections, including close visual and hammering inspections, are conducted every five years for tunnels to prevent long-term interruptions of the existing transportation infrastructure. However, detailed inspections involve road restrictions and work conditions at high elevations, causing problems for drivers and challenges in ensuring the safety of inspectors. Hence, to improve the frequency of the inspection, several inspection systems have been pro-

[1]Corresponding Author: Tomohiko Hayakawa, Tokyo University of Science, 6-3-1 Niijuku, Katsushika-ku, Tokyo 125-8585, Japan; E-mail: hayakawa@ishikawa-vision.org.

posed as substitutes for detailed inspections and to confirm deformation by photographing the surface of the tunnel lining. However, these systems generally require specialized inspection vehicles [3,4]; they also face limitations such as slow driving speed during imaging compared to the legal speed limit on expressways [5] and the need for global navigation satellite system (GNSS) calibration for each image acquisition [6].

Whereas, a tunnel inspection device [7] was proposed that can be mounted on a road patrol vehicle to enable tunnel inspection during daily patrols. This device can capture images while compensating for motion blur and discover cracks of width 0.2 mm in tunnel ceilings at a distance of 2–5 m, while traveling at 100 km/h. However, its high spatial resolution comes with the trade-off that its field of view is limited, and compensating for the orientation of the inspection camera against changes in the driving position caused by the driver's operation is required to reliably capture known cracks. Both GNSS and odometer-based solutions are inadequate for addressing the problem at hand. GNSS cannot be utilized within tunnels, while odometers have errors of a few percent, which can be influenced by variables such as speed, tire condition, and barometric pressure.

Therefor vision-based localization was conducted to obtain the driving position in real-time and control the orientation of the inspection camera. This research proposed a method for localization estimation by recognizing the lighting facilities in the tunnel using the device illustrated in Fig. 1. This device has two cameras to inspect tunnel visually and recognize road for localization, and the rotary actuator to change the angle of view to allow capturing the entire wall surface. Its feasibility for practical scenarios in the expressway tunnel inspection is validated.

2. Related Research

Lane recognition is a vehicle localization estimation method that has found applications in various fields of advanced driver-assistance systems (ADAS) such as automatic driving, with ongoing research in these fields. Light detection and ranging (LiDAR) [8,9] conducts 3D measurements by conducting 1D or 2D scanning with a rotating mirror for 1D information in the depth direction. Thus, increasing the scanning density for interrupted or adjacent lanes requires increasing the number of scans or installing a large number of LiDAR devices. However, a higher scanning density requires more time for scanning and also increases the latency between the start and end of scanning, making accurately measuring objects moving at high speeds difficult. Therefore, LiDAR is not

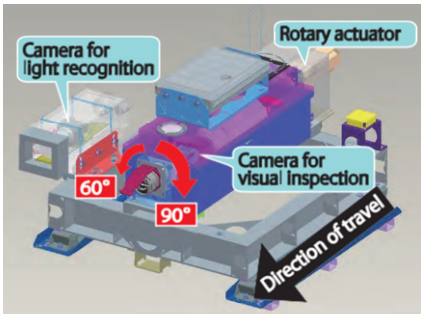

Figure 1. Overview of the inspection device for mounting on a patrol vehicle.

suitable for use on expressways. The development of solid-state LiDAR without rotating parts has shown progress, but the standard frame rate is 30 Hz or less, and emphasis is placed on improving reliability. Millimeter-wave radar [10] does not require mechanical movement for 3D scanning and can perform stable measurements at a distance of 100 m or more under varying environmental conditions. However, unlike LiDAR, which can simultaneously acquire luminance values and depth information, only the shape is measured; thus, its application conditions are limited. Moreover, a special lane with a reflective convex part (rib) is required for lane recognition, and the data update speed takes approximately several tens of milliseconds.

Vision-based lane recognition is originally affected by the brightness of the sun and weather [11]; however, it is unaffected in tunnels and is suitable for imaging. Eliminating the need for specialized vehicles requires a method that does not require camera calibration for loading and unloading equipment. The method by Adachi et al. [12] achieves vehicle localization under simple conditions without using camera parameters; however, in an actual expressway tunnel, recognizing lanes in a stable manner is challenging because of the co-existence of multiple lanes and dashed lines. Methods for dealing with diverse environments on expressways were proposed in a study by Hayakawa et al. [13], but it is not applicable in places where the lane becomes blurred due to aging or dirt. Although recognizing method of damaged stop lanes is proposed by Ito et al. [14], the method cannot correspond with complete disappearance of the lanes. Hence, more stable localization estimation method is required.

Lighting facilities are installed in tunnels and have features similar to those of lanes. In recent years, exhaust gas regulations and the shift to electric vehicles (EVs) have enabled cleaner air inside tunnels, thereby resulting in cleaner lighting covers, and partial lights are no longer turned off owing to dimming control by switching to LED lighting. Thus, lighting features can be used as stable features instead of lanes.

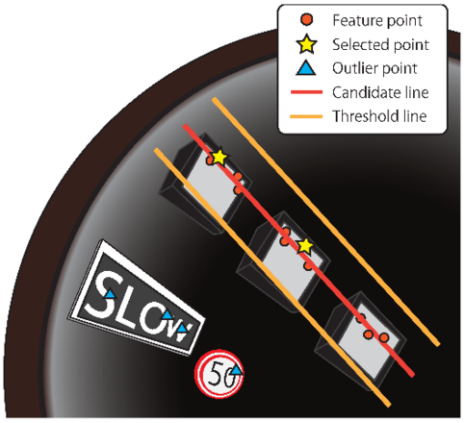

Figure 2. Overview of lighting recognition using RANSAC

3. Principle

3.1. Lighting Recognition

Lighting recognition enables real-time self-localization of vehicles and dynamically adjusts the inspection area based on their position. Lighting installed in rows on tunnel ceilings, at a certain height from the road surface, can be treated as a straight dotted line because expressway tunnels are typically designed with minimal curvature to maintain driving speed. This is recognized as two straight lines in the same manner as in lane recognition.

First, feature points are extracted from the image acquired by the forward-facing camera in Fig. 1. Unlike lanes, lighting produces equal strength edges on the long and short sides, detected using horizontal differentiation filter. Therefore, diagonal edges are obtained using the following linear filters on the left and right sides of the image:

$$F_L = \begin{pmatrix} 0 & -p & 0 & 0 \\ p & 0 & -p & 0 \\ 0 & p & 0 & -p \\ 0 & 0 & p & 0 \end{pmatrix}, \tag{1}$$

$$F_R = \begin{pmatrix} 0 & 0 & -p & 0 \\ 0 & -p & 0 & p \\ -p & 0 & p & 0 \\ 0 & p & 0 & 0 \end{pmatrix} \tag{2}$$

The obtained edge images' brightness, which changes from dark to light above a certain threshold, is extracted as a feature point. Since these feature points contain disturbances, fitting to a linear model is performed to eliminate their influence. By using random sample consensus (RANSAC) [15], it is possible to efficiently exclude disturbances and recognize illumination robustly with a small amount of computation.

As shown in Fig. 2, straight line fitting using RANSAC involves randomly selecting two points from among the feature points (red circles in Fig. 2) and setting the parameters of the straight line passing through those two selected points (yellow stars in Fig. 2) as candidates. The count of the feature point group G that is at a distance from this straight line that is less than or equal to the threshold is set as c (orange lines in Fig. 2). The G that maximizes the c is obtained through multiple trials, and a straight line from the feature points contained in G is obtained using the least squares method. Thus, only the feature points with the disturbance removed can be fitted to the straight line model. If this trial is performed on n feature points obtained from the image, then all combinations will be ${}_nC_r$. RANSAC guarantees that a correct fitting result can be obtained with probability p in N trials, as represented by (3), where e is the probability that a feature point is an outlier.

$$N = \frac{\log(1-p)}{\log(1-(1-e^2))} \tag{3}$$

3.2. Localization Estimation

Localization estimation involves recognizing the left and right lighting as straight lines; this can be achieved based on the method reported by Adachi et al., [12] as demonstrated in the following section, and updated for lightning recognition as shown in Fig. 3.

First, a homography matrix is obtained, which transforms the intersections of the left and right straight lines and the top and bottom straight lines of the image to coordinates normalized to (0,0), (1,0), (0,1), and (1,1). Furthermore, assuming that the camera is horizontal to the road surface, the straight lines at the left and right edges of the images are perpendicular to the road surface. The two straight lines contain the legs of the trapezoid representing the field of view of the camera on the road surface. By transforming them into a normalized coordinate system using the obtained homography matrix, the X coordinate of the intersection of the two straight lines indicates the position of the camera relative to the illumination. Even if the camera is tilted forward or backward, this intersection will only move along the Y axis, while the X coordinate remains the same. Thus, the camera position can be estimated accurately, even with the camera tilted upward or the limited region of interest (ROI) capturing only lighting near the vehicle.

The obtained camera position is the relative position wherein the left lighting is 0 and right lighting is 1, and this can be used to determine the rotation for photographing cracks while considering the actual dimensions in the tunnel and the mounting position of the camera. Additionally, camera parameters are not required for localization, eliminating the need for camera calibration in lighting recognition.

3.3. High-Speed Implementation

This algorithm was implemented in C++, with the upper half of the 1280 × 1024 image defined as the ROI for localization. The average process time was 10 ms. This time was not sufficient for LiDAR, which requires a long time for scanning. The bottlenecks encountered were 1) image filtering, 2) feature point extraction, and 3) RANSAC, which were all highly parallel processes. However, in case inspection and self-location estimation are performed on the same PC, large number of multi-threading may affect the performance of inspection. Hence, optimization of individual bottleneck is desirable. The

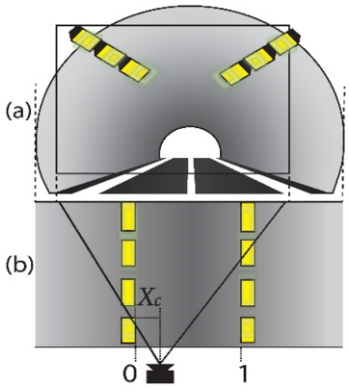

Figure 3. Relationship of lighting facilities and camera in normalized coordinate system. X_c indicates the distance between left-side lighting and a camera.

proposed method utilized the filter feature, the data structure was optimized, and single instruction/multiple data (SIMD) conversion was utilized using built-in functions to boost the speed.

3.3.1. *Improvement of Computational Efficiency of Image Filtering*

The filter F_L for the left side of the image was considered. As shown in Eq. 1, each coefficient p was any real number, so this value can be set to ± 1 by adjusting the threshold value for extracting a feature point. Essentially, the result can be obtained only by addition and subtraction of integers of six elements, and the computation amount can be greatly reduced compared to performing convolution as a 4×4 linear filter. Furthermore, based on SIMD, with one command, multiple pixels in the horizontal direction are read from memory simultaneously as vector data (a), the column position is shifted by shifting the number of bytes according to the row, and the results of conducting four vector additions and one vector subtraction are written to memory. As the shift fills the outside of the range with 0, we used a command that simultaneously reads out the pixels further behind and concats and shifts the two vectors (b). Additionally, a possibility of overflow exists due to addition (c) and subtraction (d); thus, the shifted result is converted to an integer type that is one value larger to ensure accuracy. Arithmetic right shift is conducted on the final addition/subtraction result to a degree sufficient for comparison with the threshold, and by converting to the original integer type with a pack instruction with saturation processing, the resulting edge image has the same size as the input image. A schematic diagram of vector operation about F_L is shown in Fig. 4. Herein, processing is conducted in parallel with four pixels, thus, only 62.5% of the read data is used, which is inefficient. However, when using 256-bit SIMD instructions such as advanced vector extensions (AVX) for an image with eight bits per pixel, addition and subtraction are performed in 16 bits. Thus, 16 pixels are processed in parallel, and by conducting loop unrolling once, pack instructions and writing to eight bits can allow for parallel processing of 32 pixels. At this time, 128-bit vector readout is conducted twice per row, and 32-bit scalar readout and conversion to 128-bit are conducted once. Consequently, the

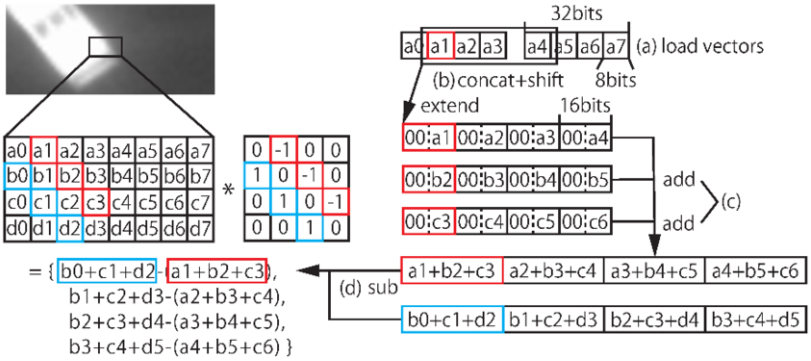

Figure 4. Schematic diagram of vector operations using SIMD equivalent to conventional matrix calculation about F_L.

efficiency of data reading during parallel processing has been significantly improved to approximately 91.7% (91.7% − 62.5% = 29.2% improvement).

3.3.2. Feature Point Extraction

In terms of feature point extraction, SIMD conversion was applied by comparing the filtering results with a threshold value. Note that, when storing the coordinates of the feature points in an array, the data structure must be set either as an array of two-dimensional vectors (i.e., array of structures (AoS)) or a structure with an array of X coordinates and an array of Y coordinates (i.e., structure of arrays (SoA)). [16]

3.3.3. RANSAC

SIMD conversion of RANSAC is parallelized for each candidate straight line. Linear parameters require floating-point arithmetic, and eight elements can be processed in parallel when handling 32-bit single precision with 256-bit SIMD commands. Therefore, combinations of two feature points selected by random numbers are handled in parallel with eight candidates. The operations for each candidate are independent, which allows for a simpler and more efficient parallelization of the aforementioned data structure (SoA). Moreover, AoS is more advantageous than SoA in processes involving reading the coordinates of feature points from an array using random numbers as indices. This is due to the limitation of AVX2 gather instructions. The gather instructions specify an index with vector data and reads out data at an arbitrary position from the array at once. If random numbers are generated and used as indices, the coordinates of candidate feature points can be read at high speeds as vector data. However, in AVX2, 256-bit gather instructions can only be conducted on eight 32-bit elements, four 64-bit elements, or two 128-bit elements. As 16-bit integers for each of the X and Y coordinates are sufficient for the coordinates of the feature point due to the size of the image, data for one feature point can be represented by 32 bits. Therefore, storing the coordinates of feature points in an array in 32-bit units as AoS enabled optimal reading using the gather command. Considering these advantages, we assumed the strategy of reading AoS data from memory and then converting it to SoA.

Consequently, the processing time was 1.2 ms on average, which was 8 times faster than the original method without high-speed implementation, and sufficiently faster than LiDAR and millimeter-wave radar.

4. Experiments

The availability of the proposed method is verified in the real environment. Through this experiment, the accuracy of the local estimation is evaluated and discussed.

4.1. Experiment Condition

As mentioned previously, this experiment is conducted in the real environment, Chuo Expressway Enasan Tunnel, and at three points on the driving lane side, which featured the crack to be inspected. The Enasan Tunnel completion drawing is shown in Fig. 5.

As an evaluation experiment of the proposed method, images were captured by two cameras for lighting recognition (SP-5000M-CXP4, JAI) and visual inspection (SP-

12000M-CXP4-XT, JAI). while the vehicle was halted within area in the expressway tunnel, and simultaneously, the distance from the device to the tunnel lining was measured using a distance sensor (DT50-2, SICK) mounted on the inspection device.

4.2. Lighting Recognition Results

First, localization estimation was conducted on the captured image using the line fitting in the proposed method as shown in Fig. 6 (a) and (b). Even if the lorry is appeared, the recognition was successful; However, in case the lorry blocks all the lighting facilities, the recognition will be failed. This point is discussed in Sec. 5.

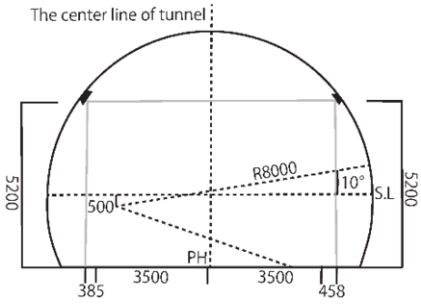

Figure 5. Tunnel dimensions around crack.

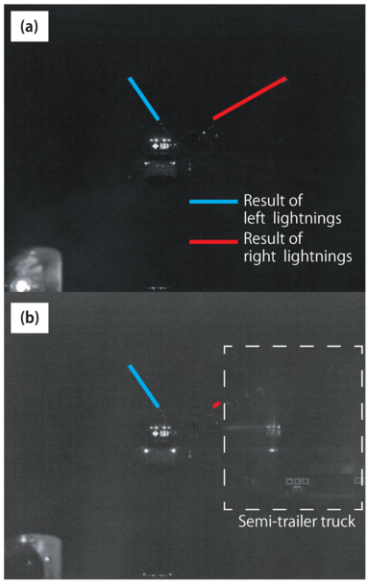

Figure 6. Line fitting results with recognized left and right straight line at crack 1. (a) Without adjacent vehicles. (b) With an adjacent lorry.

4.3. Local Estimation Results

4.3.1. Preparing the Distance Value to Compare

It is desirable to obtain the true value of the lighting position from a stopped inspection vehicle through three-dimensional measurement for the left and right lighting using a laser. However, as an active sensing method using a laser could be dangerous for general vehicles, fully restricting the road is necessary to measure. To enable a comparison with the localization estimation value, the distance between the measurement object and the camera was separately measured in order to determine the accuracy of the distance sensor's measured value; the distance from the tunnel center to the tunnel side was calculated based on the tunnel completion drawing.

Subsequently, a 3D model of the general shape of the tunnel and the lighting dimensions and installation positions was created based on the tunnel completion drawing, and the lighting observed using the camera of the inspection device was reproduced as a CG-rendered image. Using these parameters as initial values, a exhaustive search for (x, y) and $(pitch, yaw)$ was performed by template matching, setting the ROI as the area in the images where the lighting is visible. Thereafter, localization estimation involves calculating the horizontal distance from the tunnel center to the camera based on the distance between the left and right lighting. In particular, as the measured value of the distance sensor is the distance from the tunnel wall to the distance sensor, direct comparisons could not be performed. However, the total value of both is expected to be constant, regardless of the vehicle position. Additionally, by taking into account the mounting position of the distance sensor, it became possible to compare the overall value between the distance from the tunnel center to the tunnel side.

4.4. Experiment Results

Table 1 summarizes the numerical values at each point. a) is distance between device and tunnel center by the proposed localization estimation, b) is true distance value described in 4.3.1, c) is distance between device and tunnel side measured by a distance sensor. First, the comparison with CG values reveals that the maximum error is 31 mm at crack 3 between Tab. 1 a) and b). Additionally, Table 1 d) are 4,990 mm, 4,972 mm, and 4,980 mm, which are each within a maximum difference of 11 mm between the average value of 4,981 mm of the three values and d) at crack 2.1 d) at crack 2. The theoretical value T of d), the distance between the tunnel center and tunnel side, is obtained by the following equation (4) from the tunnel completion drawing, assuming that the camera height is the same as the springline height.

$$\begin{aligned} T &= \sqrt{8000^2 - 500^2} - \frac{500}{\tan 10^\circ} \\ &\simeq 5149 \end{aligned} \tag{4}$$

The theoretical value of the d) value is 5,149 mm, with a maximum difference of 177 mm from Tab. The comparison with CG values (Tab. 1 b)) and the stability of the total value (Tab. 1 d)) indicate that the localization estimation was successful, with an error in the order of several centimeters. The horizontal field of view of the inspection camera

is 528 mm at a distance of 5,000 mm ahead of the camera, which suggests sufficient accuracy. Fig. 8 shows the state of lighting recognition while driving. Straight line fitting that connects the feature points of the tunnel lighting is conducted at correct positions on the left and right, enabling localization to be stably estimated.

Table 1. Accuracy Verification Compared to Measured Values

Point	a) Estimated value [mm]	b) Pseudo true value [mm]	c) Measured distance [mm]	d) a+c [mm]
Crack1	1731	1712	3259	4990
Crack2	2334	2342	2638	4972
Crack3	2396	2365	2584	4980

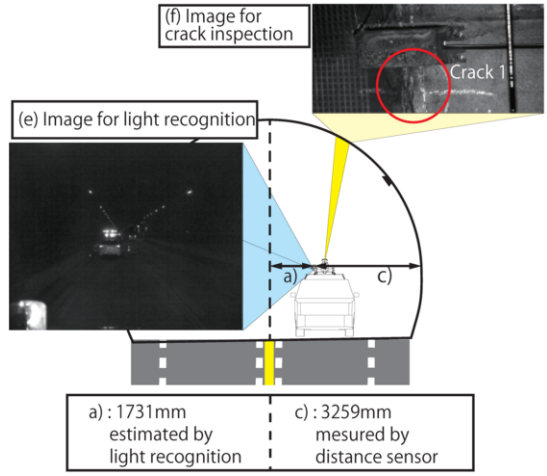

Figure 7. Experimental results in parked condition at crack 1 in Table. 1; each images are level-corrected to improve the image visibility for humans.

5. Discussion

As shown in Fig. 6 (b), a lorry did not cause decrease of accuracy to recognize lighting facilities; however, in case the lorry blocks all of them, one of the fitting lines will disappear totally, and cause a severe recognition error. To validate the error rate of the phenomenon, Fermi estimation was implemented instead of actual measurement because of limited time of the traffic restriction. 25,000 * 0.38 = 9,500 vehicles per day between the exits across the Enasan Tunnel, or 0.11 large vehicles per second [17]. If lorries were equally spaced in both lanes, the distance between lorries in the overtaking lane would be 100 [km/h] / (0.11/2) [vehicles/s] = 505 [m]. Probability of lorries per unit length is 1 / 505 [m] = 0.00198 [units/m]. Suppose the location where the lorry fails to be present is 10m in front of the patrol vehicle. Probability of a lorry being there 0.00198 * 10 = 1.98 %. Namely, the error occurs only once in 50 times.

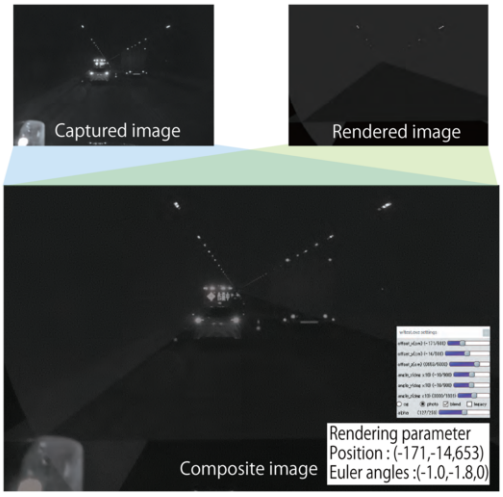

Figure 8. The result of alignment by CG at crack 1.

Additionally, the estimation values from lighting estimation based on three points with the CG alignment result constructed from the tunnel drawing had a maximum error of 31 mm, whereas a maximum error of 11 mm was derived based on the average value of the three points. Moreover, the theoretical value of the total value calculated from the tunnel completion drawing was 5,149 mm, with a maximum difference of 177 mm from the total value.

The difference between the theoretical value and measured value is likely attributed to the difference between the actual tunnel and the completion drawing due to factors such as tunnel deformation. Additionally, the tunnel is not a perfect circle; however, rather a slightly crushed ellipse; thus, the radius shown in the completion drawing is not constant. This finding indicates that the results of accurate on-site measurements should be prioritized over the completion drawings when actually operating the system. Although a distance sensor was attached to the device for verification purposes in this experiment, this equipment is essentially unnecessary. Thus, this equipment should be removed to simplify the device configuration and reduce power consumption.

6. Summary

This study proposed a stable and high-speed vision-based localization estimation method that solved the problem of lane recognition in tunnel environments on Japanese expressways where GNSS is not applicable. This was achieved by recognizing the lighting facilities installed in tunnels.

The proposed method only conducted localization estimation in the horizontal direction; however, localization estimation could be performed in the traveling direction at high speeds by counting and tracking each lighting on a recognized straight line. As the cracks to be inspected were located at various positions in the tunnel, the camera angle must be accurately pointed toward a specific crack at an arbitrary timing and angle while driving. The combined strategy of lighting recognition and lighting counting proposed in this study enables more frequent inspections of the tunnel lining to detect cracks that lead

to flaking. Thus, this strategy can enhance tunnel infrastructure safety while reducing costs. Overall, the study offers an innovative and efficient solution for tunnel inspection.

References

[1] Road Subcommittee, National Road Committee, Council for Social Infrastructure, Ministry of Land, Infrastructure, Transport and Tourism, Interim report, URL: https://www.mlit.go.jp/report/press/content/001417808.pdf (accessed 2023-05-10).

[2] J. A. Richards: Inspection, maintenance and repair of tunnels: International lessons and practice, Tunn. Undergr. Sp. Technol., Vol.13, No.4, pp.369–375, 1998.

[3] T. Yasuda, H. Yamamoto, and Y. Shigeta, "Tunnel Inspection System by using High-speed Mo- bile 3D Survey Vehicle: MIMM-R,"J. of the Robotics Society of Japan, Vol.34, No.9, pp. 589-590, doi:10.7210/jrsj.34.589, 2016.

[4] S. Nakamura, A. Yamashita, F. Inoue, D. Inoue, Y. Takahashi, N. Kamimura, T. Ueno, Inspection Test of a Tunnel with an Inspection Vehicle for Tunnel Lining Concrete, Journal of Robotics and Mechatronics, Vol.31, No.6, pp. 762-771, 2019.

[5] Tunnel Inspection System for General Vehicles registered with NETIS: URL: https://jp.ricoh.com/-/Media/Ricoh/Sites/jp_ricoh/release/2019/pdf/1112_1.pdf (accessed 2023-05-19).

[6] K. Suzuki, H. Yamaguchi, K. Yamamoto, and N. Okamoto, Tunnel inspection support service using 8K area sensor camera, J. of the Japan Society of Photogrammetry, Vol.60, No.2, pp. 40-41, doi: 10.4287/jsprs.60.40, 2021.

[7] T. Hayakawa, Y. Moko, K. Morishita, and M. Ishikawa, Pixel-wise deblurring imaging system based on active vision for structural health monitoring at a speed of 100 km/h, In Tenth International Conference on Machine Vision (ICMV 2017), vol. 10696, pp. 548-554. SPIE, 2018.

[8] T. Ogawa and K. Takagi, Lane Recognition Using On-vehicle LIDAR, 2006 IEEE Intelligent Vehicles Symposium, 2006, pp. 540-545.

[9] A. Von Reyher, A. Joos, and H. Winner, A lidar-based approach for near range lane detection, in Proceedings of IEEE Intelligent Vehicles Symposium 2005, pp. 147-152, 2005.

[10] Y. Song, Z. Xie, X. Wang and Y. Zou, MS-YOLO: Object Detection Based on YOLOv5 Optimized Fusion Millimeter-Wave Radar and Machine Vision, in IEEE Sensors Journal, vol. 22, no. 15, pp. 15435-15447, 1 Aug.1, 2022, doi: 10.1109/JSEN.2022.3167251.

[11] J. Wang, K. Wan, C. Pang and W. Yau, Semi-Supervised Image-to-Image Translation for Lane Detection in Rain, in Proceedings of 2022 IEEE 25th International Conference on Intelligent Transportation Systems (ITSC), pp. 118-123, 2022

[12] J. Adachi and J. Sato, Estimation of vehicle positions from uncalibrated cameras, The IEICE Trans. on Information and Systems (Japanese edition), Vol.D89, No.1, pp. 74-83, 2006.

[13] T. Hayakawa, Y. Moko, K. Morishita, Y. Hiruma, M. Ishikawa, Tunnel Surface Monitoring System with Angle of View Compensation Function based on Self-localization by Lane Detection, Journal of Robotics and Mechatronics, Vol. 34, No. 5, pp. 997-1010, 2022.

[14] T. Ito, , K. Tohriyama, and M. Kamata, Detection of Damaged Stop Lines on Public Roads by Focusing on Piece Distribution of Paired Edges, Int. J. ITS Res. 19, pp. 56-70, 2021.

[15] M. A. Fischler and R. C. Bolles, Random sample consensus: A paradigm for model fitting with applications to image analysis and automated cartography, Communications of the ACM, vol. 24, no. 6, pp. 381–395, 1981.

[16] J. Abel, K. Balasubramanian, Applications tuning for streaming SIMD extensions, Intel Technology Journal Q 2 (1999): 1999.

[17] K. Goto, T. Tominaga, H. Amano, S. Aoki, Deck Slab Replacement Work that Realized Rapid Construction by Applying New Technologies, Concrete Journal, Vol. 58, No. 4, pp. 297-302, 2021.